

Tunable singlet-triplet splitting in a few-electron Si/SiGe quantum dot

Zhan Shi, C. B. Simmons, J. R. Prance, John King Gamble, Mark Friesen et al.

Citation: *Appl. Phys. Lett.* **99**, 233108 (2011); doi: 10.1063/1.3666232

View online: <http://dx.doi.org/10.1063/1.3666232>

View Table of Contents: <http://apl.aip.org/resource/1/APPLAB/v99/i23>

Published by the [American Institute of Physics](#).

Related Articles

Anisotropy of electron and hole g-factors in (In,Ga)As quantum dots

Appl. Phys. Lett. **99**, 221914 (2011)

Entanglement generation and quantum state transfer between two quantum dot molecules mediated by quantum bus of plasmonic circuits

Appl. Phys. Lett. **99**, 223509 (2011)

Al-doped ZnO nanocrystals: Electronic states through scanning tunneling spectroscopy

J. Appl. Phys. **110**, 104303 (2011)

In-plane polarization anisotropy of ground state optical intensity in InAs/GaAs quantum dots

J. Appl. Phys. **110**, 094512 (2011)

Dynamics of interatomic Coulombic decay in quantum dots

J. Chem. Phys. **135**, 144112 (2011)

Additional information on *Appl. Phys. Lett.*

Journal Homepage: <http://apl.aip.org/>

Journal Information: http://apl.aip.org/about/about_the_journal

Top downloads: http://apl.aip.org/features/most_downloaded

Information for Authors: <http://apl.aip.org/authors>

ADVERTISEMENT

**AIP**Advances

Submit Now

**Explore AIP's new
open-access journal**

- **Article-level metrics
now available**
- **Join the conversation!
Rate & comment on articles**

Tunable singlet-triplet splitting in a few-electron Si/SiGe quantum dot

Zhan Shi, C. B. Simmons, J. R. Prance, John King Gamble, Mark Friesen, D. E. Savage, M. G. Lagally, S. N. Coppersmith, and M. A. Eriksson^{a)}
 University of Wisconsin-Madison, Madison, Wisconsin 53706, USA

(Received 1 September 2011; accepted 9 November 2011; published online 8 December 2011)

We measure the excited-state spectrum of a Si/SiGe quantum dot as a function of in-plane magnetic field and identify the spin of the lowest three eigenstates in an effective two-electron regime. We extract the singlet-triplet splitting, an essential parameter for spin qubits, from the data. We find it to be tunable by lateral displacement of the dot, which is realized by changing two gate voltages on opposite sides of the device. We present calculations showing the data are consistent with a spectrum in which the first excited state of the dot is a valley-orbit state. © 2011 American Institute of Physics. [doi:10.1063/1.3666232]

Silicon quantum dots are candidate hosts for semiconductor spin qubits. Long spin relaxation times have been demonstrated in Si quantum dots and donors,^{1–4} and measurements of ensembles of donor-bound spins by electron spin resonance have demonstrated T_2 coherence times up to 2 s.⁵ One of the key properties of Si quantum dot spin qubits is the ability to tune in real-time tunnel rates and couplings between neighboring dots by controlling electrostatic gate voltages.^{6–8} Tunable, gate-defined Si quantum dots often are designed to sit at the interface between pure Si and a barrier of either SiGe (Refs. 9 and 10) or SiO₂ (Refs. 11–13).

An essential parameter for singlet-triplet qubits is the energy difference E_{ST} between the singlet (with both electrons occupying the lowest energy single-particle state) and triplet states (built out of the lowest energy single-particle state and the first excited state) of two electrons in one dot.^{14,15} The energy E_{ST} is equal to the lowest single-particle excited state energy minus a correction arising from electron-electron interactions. In Si nanostructures, which have states arising from the two low-lying valleys in the Si conduction band, the interface between Si and the barrier material plays an important role in determining this energy.¹⁶ Experiments have shown that quantum-confined structures can have valley splittings ranging from 100 μ eV to 1–2 meV.^{17–19} The existence of large valley splitting in Si quantum dots has led to large E_{ST} and the observation of Pauli spin blockade.^{20,21} However, systematic control of the valley splitting or, more directly, E_{ST} has not been demonstrated in a Si quantum dot.

In this letter, we report a magnetospectroscopy study of a Si/SiGe double quantum dot with 2 and 0 valence electrons on the left and right dots, respectively. We measure the evolution of the ground and low-lying excited states of the left dot as a function of an in-plane magnetic field B . We extract the magnetic field B_{ST} at which the ground state changes from singlet to triplet, corresponding to the Zeeman energy equaling the singlet-triplet splitting E_{ST} for the (2,0) charge configuration. We find that B_{ST} is tunable by lateral displacement of the quantum dot location, achieved by changing two

gate voltages on opposite sides of the dot. B_{ST} evolves systematically as a function of the gate voltages, and we measure a fractional change in B_{ST} of up to 19%. Changes in gate voltages can alter both the position and shape of the electron wavefunctions in quantum dots.^{22–24} Applying asymmetric changes to voltages on either side of a quantum dot, as we do here, will change primarily the dot position. We perform calculations showing that the change in B_{ST} observed is consistent with valley-orbit mixing arising from a rough Si/SiGe interface.

A double quantum dot, shown in Fig. 1(a), is fabricated as described in Ref. 2. A quantum point contact (QPC), defined by gates R and Q, is used to perform charge sensing measurements. Gate L is connected to a pulse generator (Tektronix AFG3252), allowing the application of fast voltage pulses. The dc gate voltages are tuned so that the double dot is in the few-electron regime, as shown in Fig. 1(b). The change in background grayscale arises from changes in the QPC sensitivity caused by capacitive cross-talk in the device.²⁵ Measurements are performed in a dilution refrigerator at an electron temperature $T_e = 143 \pm 10$ mK, determined as described in Ref. 2. The electron occupation numbers are effective; we believe there are spin-zero closed shells of electrons in both the left and the right dots that do not participate in the physics discussed here.

To determine the 2-electron singlet-triplet splitting, we measure the gate voltage dependence of the transition from a

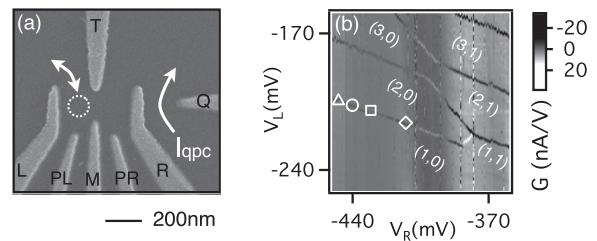


FIG. 1. (a) SEM image of a double dot identical to the one used in the experiment. The transition measured here is between the left dot (white circle) and the left reservoir. (b) Stability diagram of the double dot with effective electron occupation numbers labeled. The white symbols between regions (1,0) and (2,0) correspond to the gate voltages for the data reported below in Fig. 3. The line between (1,0) and (1,1) is invisible because of a slow tunnel rate.

^{a)} Author to whom correspondence should be addressed. Electronic mail: maeriksson@wisc.edu.

single-electron spin-down state to the 2-electron ground state as a function of B . Figs. 2(a) and 2(b) show the transconductance $G = \partial I_{\text{qpc}} / \partial V_L$ as a function of B , measured with a lock-in amplifier using a $120 \mu\text{V}$ ac excitation voltage applied to gate L. The bright peak in the color plot corresponds to adding one electron to the left dot. The gate voltage of this transition first increases and then decreases as a function of B .

The electrochemical potential μ_N has a dependence on the in-plane magnetic field of the form $\partial \mu_N / \partial B = g \mu_B \Delta_{S_{\text{tot}}}(N)$.²⁶ Here g is the Landé g -factor, μ_B is the Bohr magneton, and $\Delta_{S_{\text{tot}}}(N)$ is the change in the z component of the total spin quantum number when the N th electron is added to the dot. The electrochemical potential has a slope of $+g\mu_B/2$ when a spin-up electron is added (magnetic moment antiparallel to B), whereas the addition of a spin-down electron results in a slope of $-g\mu_B/2$ (magnetic moment parallel to B). The positive slope in Figs. 2(a) and 2(b) at small B corresponds to the addition of a spin-up electron, forming a 2-electron singlet ground state. The arrows mark B_{ST} , the magnetic field at which the slope changes; for $B > B_{\text{ST}}$, the added electron is spin-down, and the ground state is the triplet T_- . As indicated in Fig. 2(c), at $B = B_{\text{ST}}$, the Zeeman energy of the state T_- is equal to $E_{\text{ST}}(B=0)$. The value of B_{ST} is different in Figs. 2(a) and 2(b), indicating that E_{ST} is tunable with gate voltage.

Pulsed-gate spectroscopy^{27,28} allows us to confirm this state identification and measures excited-states as a function of B . Square wave voltage pulses of peak-to-peak amplitude 3.6 mV and frequency 50 kHz are applied to gate L, and the

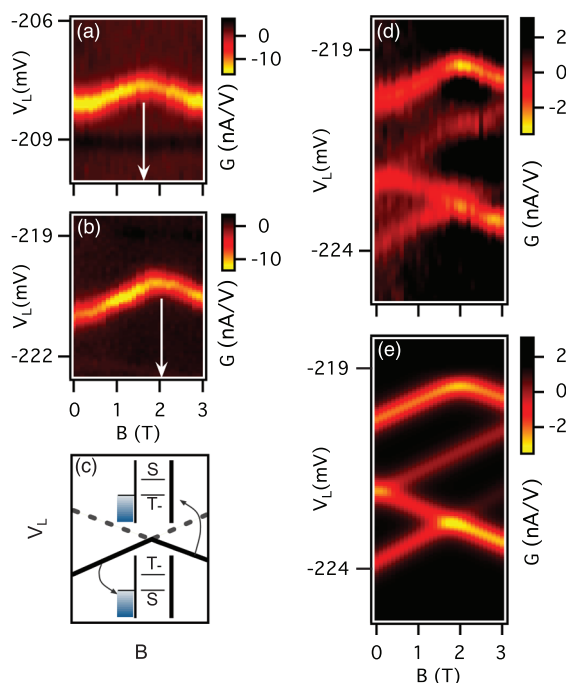


FIG. 2. (Color online) (a) and (b) Ground state spectroscopy for two different sets of gate voltages chosen so that the gate voltages for (b) favor a dot position farther to the right than those for (a) (see Fig. 3). The plots show the QPC conductance G . The arrows indicate the magnetic field B_{ST} at which the Zeeman shift for the T_- equals the zero-field E_{ST} . (c) Diagram showing the transition as a function of B . (d) Excited state spectroscopy using pulsed-gate voltages for the dot position corresponding to (b). (e) Simulated spectroscopy for the data in panel (d).

time-averaged value of G is recorded. In Fig. 2(d), the bottom (top) line, corresponds to the positive (negative) edge of the pulse bringing the ground state into resonance with the Fermi level of the lead. These lines reproduce the shape of the line in Fig. 2(b).

The two middle lines in Fig. 2(d) meet at $B = 0$ and correspond to the triplet states T_- and T_0 , which are degenerate at this point; as B increases, the lines split. The T_- line has a negative slope, corresponding to adding a spin-down electron, and it becomes the ground state when $B = B_{\text{ST}}$. The T_0 line has positive slope, corresponding to adding a spin-up electron. There is small chance of loading the T_+ after unloading the singlet into a spin-up state; however, the process is weak and produces a line at the same location as T_0 .

Fig. 2(e) shows a simulation of the experiment of Fig. 2(d) performed using a coupled rate equation model similar to that in the supplemental material for Ref. 2. The model includes thermal broadening but neglects energy-dependent tunneling. The S , T_0 , and T_- loading and unloading rates are determined by fitting the simulation to the data in Fig. 2(d). We find the loading rates $\Gamma_S^L = 45.1 \text{ kHz}$, $\Gamma_T^L = 216 \text{ kHz}$, and $\Gamma_{T_0}^L = 377 \text{ kHz}$, and the unloading rates $\Gamma_S^U = 164 \text{ kHz}$, $\Gamma_T^U = 354 \text{ kHz}$, and $\Gamma_{T_0}^U = 183 \text{ kHz}$.

Using the method illustrated in Figs. 2(a) and 2(b), we measure the transition field B_{ST} at four different gate voltage configurations, corresponding to the symbols shown in Fig. 1(b). Along this line in the stability diagram, changes in V_L and V_R tend to shift the dot physically from left to right as V_R (V_V) is made more positive (negative). As shown in Fig. 3, we observe a systematic increase in B_{ST} as we move from left to right in the stability diagram: B_{ST} increases from $1.68 \pm 0.09 \text{ T}$ to $2.02 \pm 0.07 \text{ T}$, a total increase of $\sim 19\%$.

The singlet-triplet splitting can be expressed as $E_{\text{ST}} = E_1 - E_0 + C_{01} - C_{00} + K_{\text{ST}}$, where E_0 and E_1 denote the ground and first excited-state energies, C_{00} and C_{01} are the Coulomb interaction energies of the two electrons in the singlet and triplet states, and K_{ST} is the exchange energy.²⁹ A simple shift of the dot position is expected to have little effect on the last three terms, which correspond to interactions between the electrons. Similarly, the wavefunction envelope should change little as the dot is displaced. The variation in B_{ST} is not caused by a change in g -factor as a function of gate voltage, because we calculate that only 0.6% of the electron density resides in the SiGe barrier, and the g -factor changes $\sim 2\%$ between Si and the $\text{Si}_{0.7}\text{Ge}_{0.3}$ used here.³⁰

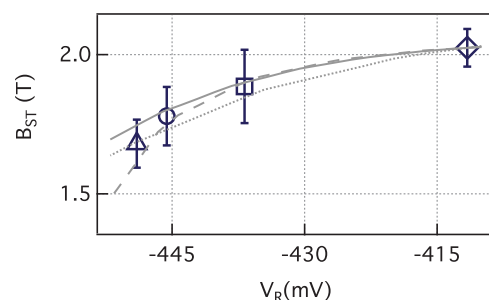


FIG. 3. (Color online) B_{ST} , the magnetic field at which the ground state shifts from S to T_- , for different sets of V_L and V_R , corresponding to the symbols on the stability diagram in Fig. 1(b). Error bars are determined by the uncertainty in linear fits to lines like those in Figs. 2(a) and 2(b). The three lines show fits with different sets of microscopic parameters.

The single-particle spacing $\Delta E = E_1 - E_0$ has a contribution arising from the difference in valley components in the two lowest lying orbital states. The quantum well interface will have atomic steps and other sharp changes in potential that vary as a function of lateral position, and these variations modify the coupling of the z-valleys, contributing to a position dependence of ΔE .^{31,32}

To test whether atomic-scale variation can account for the observed variations in B_{ST} , we perform tight-binding calculations of the single particle energy levels of an electron confined near a single atomic step. The calculations use a two-dimensional tight-binding Hamiltonian similar to Refs. 33 and 34, including parabolic lateral confinement. The fitting procedure varies the position of the atomic step, the confinement length scale, and the vertical electric field, enabling a calculation of the variation in ΔE with gate voltage. To compare with the measured B_{ST} , we also fit the sum of the Coulomb and exchange energies ($C_{01} - C_{00} + K_{ST}$), and the results are plotted in Fig. 3. The fitting is underconstrained: there are many ways to produce similar valley splitting. To indicate the types of variations possible, three results are plotted in Fig. 3 as the solid, dashed, and dotted lines, and all three calculations can reproduce the magnitude of the observed change in B_{ST} . The lowest excited-state can be classified as “orbital-like” when the calculated wavefunction contains a lateral node or “valley-like” when it does not, and both cases occur. For valley-like excitations, translation of the dot with respect to a step results in a tunable valley splitting. For orbital-like excitations, strong valley-orbit coupling enables a tunable orbital energy splitting.³⁵ Thus, atomic-scale structure of the quantum well interface alone is sufficient to produce valley-orbit mixing large enough to account for the experimental observations.

We thank B. Rosemeyer and D. Greenheck for experimental assistance. This work was supported in part by ARO and LPS (W911NF-08-1-0482), NSF (DMR-0805045), and the United States Department of Defense. The views and conclusions contained in this document are those of the authors and should not be interpreted as representing the official policies, either expressly or implied, of the U.S. Government. This research utilized NSF-supported shared facilities at the University of Wisconsin-Madison.

¹M. Xiao, M. G. House, and H. W. Jiang, *Phys. Rev. Lett.* **104**, 096801 (2010).

²C. B. Simmons, J. R. Prance, B. J. Van Bael, T. S. Koh, Z. Shi, D. E. Savage, M. G. Lagally, R. Joynt, M. Friesen, S. N. Coppersmith *et al.*, *Phys. Rev. Lett.* **106**, 156804 (2011).

³R. R. Hayes, A. A. Kiselev, M. G. Borselli, S. S. Bui, E. T. Croke, P. W. Deelman, B. M. Maune, I. Milosavljevic, J.-S. Moon, R. S. Ross *et al.*, e-print arXiv:0908.0173.

⁴A. Morello, J. Pla, F. Zwanenburg, K. Chan, K. Tan, H. Huebl, M. Mottonen, C. Nugroho, C. Yang, J. van Donkelaar *et al.*, *Nature* **467**, 687 (2010).

⁵A. M. Tyryshkin, S. Tojo, J. J. L. Morton, H. Riemann, N. V. Abrosimov, P. Becker, H.-J. Pohl, T. Schenkel, M. L. W. Thewalt, K. M. Itoh *et al.*, e-print arXiv:1105.3772v1.

⁶N. M. Zimmerman, B. J. Simonds, A. Fujiwara, Y. Ono, Y. Takahashi, and H. Inokawa, *Appl. Phys. Lett.* **90**, 033507 (2007).

⁷C. B. Simmons, M. Thalakulam, B. M. Rosemeyer, B. J. V. Bael, E. K. Sackmann, D. E. Savage, M. G. Lagally, R. Joynt, M. Friesen, S. N. Coppersmith *et al.*, *Nano Lett.* **9**, 3234 (2009).

⁸L. A. Tracy, E. P. Nordberg, R. W. Young, C. B. Pinilla, H. L. Stalford, G. A. T. Eyck, K. Eng, K. D. Childs, J. R. Wendt, R. K. Grubbs *et al.*, *Appl. Phys. Lett.* **97**, 192110 (2010).

⁹K. A. Slinker, K. L. M. Lewis, C. C. Haselby, S. Goswami, L. J. Klein, J. O. Chu, S. N. Coppersmith, R. Joynt, R. H. Blick, M. Friesen *et al.*, *New J. Phys.* **7**, 246 (2005).

¹⁰T. Berer, D. Pachinger, G. Pillwein, M. Mühlberger, H. Lichtenberger, G. Brunthaler, and F. Schäffler, *Appl. Phys. Lett.* **88**, 162112 (2006).

¹¹S. J. Angus, A. J. Ferguson, A. S. Dzurak, and R. G. Clark, *Nano Lett.* **7**, 2051 (2007).

¹²E. P. Nordberg, H. L. Stalford, R. Young, G. A. T. Eyck, K. Eng, L. A. Tracy, K. D. Childs, J. R. Wendt, R. K. Grubbs, J. Stevens *et al.*, *Appl. Phys. Lett.* **95**, 202102 (2009).

¹³M. Xiao, M. G. House, and H. W. Jiang, *Appl. Phys. Lett.* **97**, 032103 (2010).

¹⁴J. Levy, *Phys. Rev. Lett.* **89**, 147902 (2002).

¹⁵J. R. Petta, A. C. Johnson, J. M. Taylor, E. A. Laird, A. Yacoby, M. D. Lukin, C. M. Marcus, M. P. Hanson, and A. C. Gossard, *Science* **309**, 2180 (2005).

¹⁶M. Friesen, M. A. Eriksson, and S. N. Coppersmith, *Appl. Phys. Lett.* **89**, 202106 (2006).

¹⁷S. Goswami, K. A. Slinker, M. Friesen, L. M. McGuire, J. L. Truitt, C. Tahan, L. J. Klein, J. O. Chu, P. M. Mooney, D. W. van der Weide *et al.*, *Nat. Phys.* **3**, 41 (2007).

¹⁸M. G. Borselli, R. S. Ross, A. A. Kiselev, E. T. Croke, K. S. Holabird, P. W. Deelman, L. D. Warren, I. Alvarado-Rodriguez, I. Milosavljevic, F. C. Ku *et al.*, *Appl. Phys. Lett.* **98**, 123118 (2011).

¹⁹W. H. Lim, C. H. Yang, F. A. Zwanenberg, and A. S. Dzurak, *Nanotechnology* **22**, 335704 (2011).

²⁰N. Shaji, C. B. Simmons, M. Thalakulam, L. J. Klein, H. Qin, H. Luo, D. E. Savage, M. G. Lagally, A. J. Rimberg, R. Joynt *et al.*, *Nat. Phys.* **4**, 540 (2008).

²¹H. W. Liu, T. Fujisawa, Y. Ono, H. Inokawa, A. Fujiwara, K. Takashina, and Y. Hirayama, *Phys. Rev. B* **77**, 073310 (2008).

²²J. Kyriakidis, M. Pioro-Ladriere, M. Ciorga, A. S. Sachrajda, P. Hawrylak, *Phys. Rev. B* **66**, 035320 (2002).

²³S. Amasha, K. MacLean, I. P. Radu, D. M. Zumbuehl, M. A. Kastner, M. P. Hanson, and A. C. Gossard, *Phys. Rev. Lett.* **100**, 046803 (2008).

²⁴M. Thalakulam, C. B. Simmons, B. M. Rosemeyer, D. E. Savage, M. G. Lagally, M. Friesen, S. N. Coppersmith, and M. A. Eriksson, *Appl. Phys. Lett.* **96**, 183104 (2010).

²⁵C. B. Simmons, M. Thalakulam, N. Shaji, L. J. Klein, H. Qin, R. H. Blick, D. E. Savage, M. G. Lagally, S. N. Coppersmith, and M. A. Eriksson, *Appl. Phys. Lett.* **91**, 213103 (2007).

²⁶Y. Hada and M. Eto, *Phys. Rev. B* **68**, 155322 (2003).

²⁷J. M. Elzerman, R. Hanson, L. H. W. van Beveren, L. M. K. Vandersypen, and L. P. Kouwenhoven, *Appl. Phys. Lett.* **84**, 4617 (2004).

²⁸M. Thalakulam, C. B. Simmons, B. J. V. Bael, B. M. Rosemeyer, D. E. Savage, M. G. Lagally, M. Friesen, S. N. Coppersmith, and M. A. Eriksson, *Phys. Rev. B* **84**, 045307 (2011).

²⁹R. Hanson, L. P. Kouwenhoven, J. R. Petta, S. Tarucha, and L. M. K. Vandersypen, *Rev. Mod. Phys.* **79**, 1217 (2007).

³⁰F. A. Baron, Ph.D. dissertation UCLA, 2006.

³¹M. Friesen and S. N. Coppersmith, *Phys. Rev. B* **81**, 115324 (2010).

³²D. Culcer, X. Hu, and S. Das Sarma, *Phys. Rev. B* **82**, 205315 (2010).

³³T. B. Boykin, G. Klimeck, M. A. Eriksson, M. Friesen, S. N. Coppersmith, P. von Allmen, F. Oyafuso, and S. Lee, *Appl. Phys. Lett.* **84**, 115 (2004).

³⁴A. L. Saraiva, B. Koiller, and M. Friesen, *Phys. Rev. B* **82**, 245314 (2010).

³⁵J. K. Gamble, S. N. Coppersmith, and M. Friesen, “Valley-orbit coupling in Si/SiGe heterostructures with interface disorder,” (unpublished).